Supplemental Information

Selenocysteine Substitution into a Class I Ribonucleotide Reductase

Brandon L. Greene[†], JoAnne Stubbe[‡§], and Daniel G. Nocera[#]*

[†]Department of Chemistry and Biochemistry, University of California Santa Barbara, Santa Barbara CA 93106

[‡]Department of Chemistry and [§]Department of Biology, Massachusetts Institute of Technology, Cambridge MA 20139

[#]Department of Chemistry and Chemical Biology, Harvard University, Cambridge MA 02138

[*]Email: greene@chem.ucsb.edu

Table of Contents

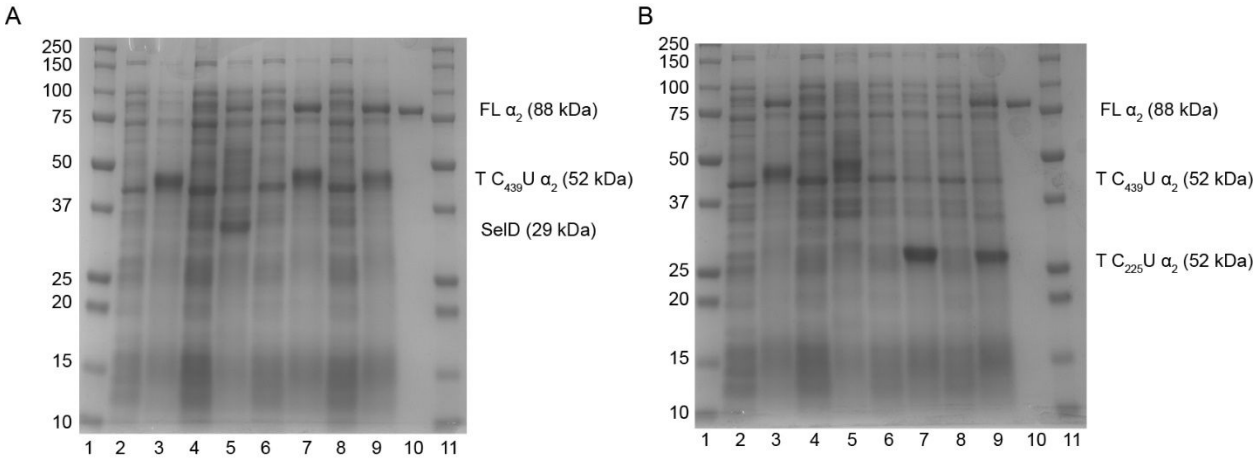

Figure S1. SDS-PAGE analysis of IPTG/arabinose dependence of $C_{439}U$ and $C_{225}U$ expression in ME6 cells. General conditions as follows; 10 mL culture inoculated with a single colony from freshly prepared plates, 100 μg/mL ampicillin, 50 μg/mL kanamycin, 30 μM Na_2SeO_3 in LB media. Arabinose (ara) added at OD_{600} = 0.5, IPTG added at OD_{600} = 0.8. Cells grown at 37 °C shaking at 200 rpm until OD = 0.5 reached, then temperature dropped to 30 °C and grown for an additional 20 h. Pre- and post-induction cell samples were collected at OD = 0.5 and OD = 4-6 respectively. **A** $C_{439}U$ expression as a function of induction conditions. *Lane 1*, molecular weight marker; *lane 2*, $C_{439}U$ 0.2 mM IPTG/0% (w/v) ara pre-induction; *lane 3*, $C_{439}U$ 0.2 mM IPTG/0% ara post-induction; *lane 4*, $C_{439}U$ 0 mM IPTG/0.1% ara pre-induction; *lane 5*, $C_{439}U$ 0 mM IPTG/0.1% ara post-induction; *lane 6*, $C_{439}U$ 0.2 mM IPTG/0.1% ara pre-induction; *lane 7*, $C_{439}U$ 0.2 mM IPTG/0.1% ara post-induction; *lane 8*, $C_{439}U$ 0.2 mM IPTG/0.2% ara pre-induction; *lane 9*, $C_{439}U$ 0.2 mM IPTG/0.2% ara post-induction; *lane 10*, authentic wt α_2 standard; *lane 11*, molecular weight marker. FL = full length; T = truncated. **B** *Lane 1*, molecular weight marker; *lane 2*, $C_{439}U$ 0.4 mM IPTG/0.2% ara pre-induction; *lane 3*, $C_{439}U$ 0.4 mM IPTG/0.2% ara post-induction; *lane 4*, $C_{439}U$ 0 mM IPTG/0 % ara pre-induction; *lane 5*, $C_{439}U$ 0 mM IPTG/0% ara post-induction; *lane 6*, $C_{225}U$ 0.2 mM IPTG/0% ara pre-induction; *lane 7*, $C_{225}U$ 0.2 mM IPTG/0% ara post-induction; *lane 8*, $C_{225}U$ 0.2 mM IPTG/0.1% ara pre-induction; *lane 9*, $C_{225}U$ 0.2 mM IPTG/0.1% ara post-induction; *lane 10*, authentic wt α_2 standard; *lane 11*, molecular weight marker.

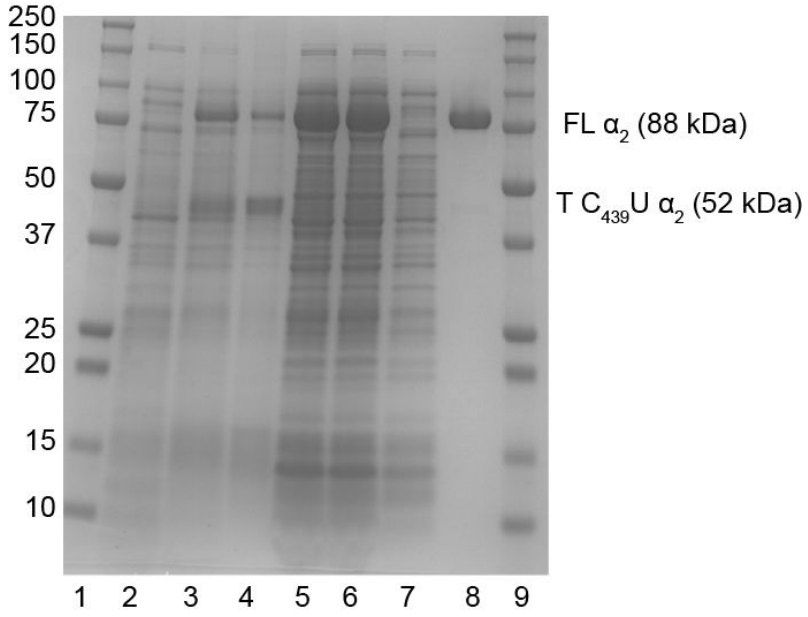

Figure S2. SDS-PAGE analysis of $C_{439}U$ purification. *Lane 1*, molecular weight marker; *lane 2*, pre-induction ME6 cells; *lane 3*, 20 h post-induction ME6 cells; *lane 4*, cell lysate debris; *lane 5*, cell lysate supernatant; *lane 6*, DNA precipitation supernatant; *lane 7*, Ni-NTA column flow-through at 50 mM imidazol; *lane 8*, eluted $C_{439}U$ α_2 (250 mM imidazole); *lane 9* molecular weight marker. FL = full length; T = truncated.

Table S1. Selenium quantitation in $C_{439}U$, $C_{225}U$, wt, and $C_{439}S$ α_2 under various expression conditions.

Protein	Expression Conditions	Yield (mg/g)	[Se]/[α]
$C_{439}U$	100 μM Na_2SeO_3 0.1% Arabinose 1 mM IPTG	9	0.54 (0.06)
$C_{439}U$	100 μM Na_2SeO_3 0.1% Arabinose 0.5 mM IPTG	4	0.70 (0.06)
$C_{439}U$	30 μM Na_2SeO_3 0.1% Arabinose 0.25 mM IPTG	1-2	1.0 (0.1)*
$C_{225}U$	30 μM Na_2SeO_3 0.1% Arabinose 0.25 mM IPTG	0.5	0.82 (0.07)
wt	30 μM Na_2SeO_3 0.1% Arabinose 0.25 mM IPTG	3.5	0.006 (0.002)
$C_{439}S$	30 μM Na_2SeO_3 0.1% Arabinose 0.25 mM IPTG	3.0	0.002 (0.003)

* Three independent preparations under these conditions have been analyzed and the error in [Se]/[α] is significantly larger among triplicate samples of a single protein preparation (+/– 9%) than among the averages of the three preparations (+/– 2%).

Table S2. Steady state and single turnover activity of wt, $C_{439}X$, and $C_{225}X$ proteins (X = S, U).

Protein	Steady State (units)	Single Turnover
wt	1920 (30)	1.6 (0.2)
$C_{439}S$	20 (20)	0.02 (0.02)
$C_{439}U$	30 (20)	0.02 (0.01)
$C_{225}U$	30 (20)	0.04 (0.04)
WT ($-O_2$, +200 μM DTT)	1900 (40)	11 (3)
$C_{439}U$ ($-O_2$, +200 μM DTT)	n.d.	0.24 (0.03)
$C_{225}U$ ($-O_2$, + 200 μM DTT)	n.d.	7.9 (0.9)

n.d., not determined

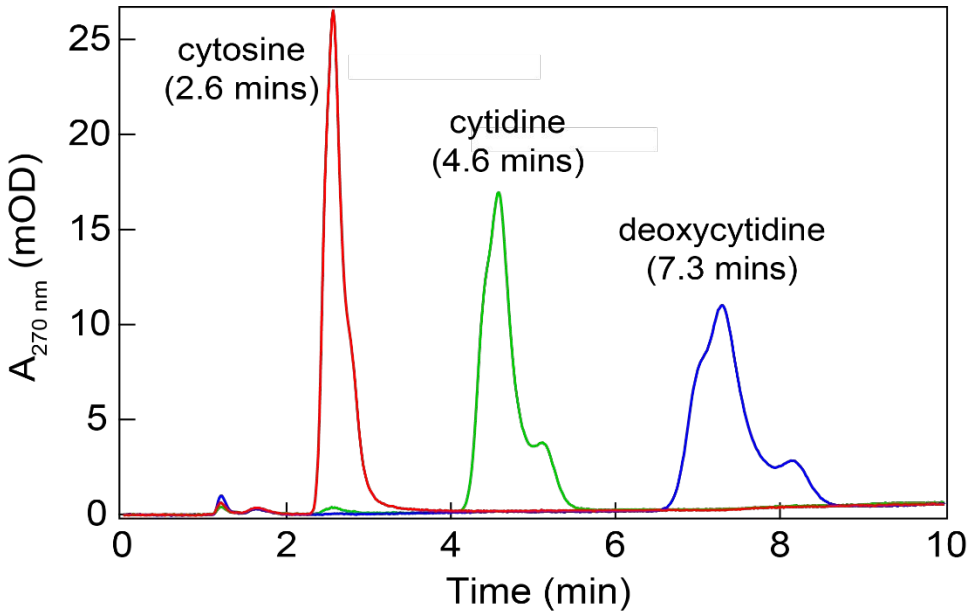

Figure S3. Individual HPLC standards for cytosine (red), cytidine (green), deoxycytidine (blue). Standards were prepared at 50 µM in 5 mM KP_i pH = 6.8. Elution gradient is identical to that reported in the materials and methods.

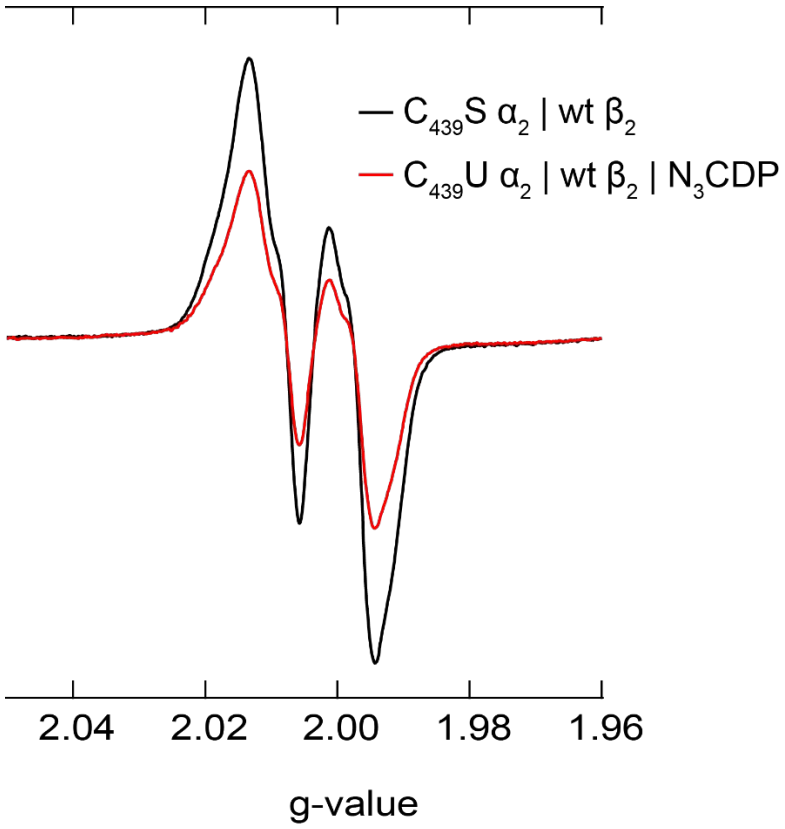

Figure S4. X-band EPR spectra of 50 μM wt β_2 with 50 μM $C_{439}S$ α_2, 1 mM CDP and 3 mM ATP (black) and 50 μM $C_{439}U$ α_2, 0.2 mM N_3CDP and 3 mM ATP (red). Spectra recorded at 80 K with 1 Gauss modulation amplitude, 100 kHz modulation frequency, and 20 μW microwave power.

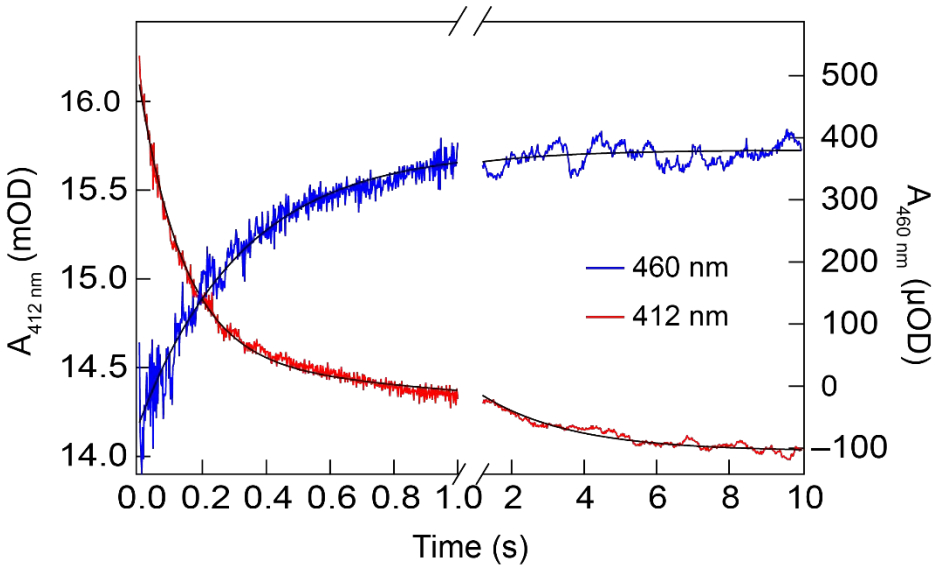

Figure S5. Stopped-flow UV-vis kinetic traces 412 nm (red, as reported in the main text), 460 nm (blue) and associated bi- and monoexponential fits respectively (black). Sample conditions identical to those of Figure 4 of the main text. The 460 nm transient was equally well fit by mono- or biexponential, likely due to the lower signal to noise, and thus the mono-exponential fit is reported. The k_{obs} = 3.19 (0.05) s^{-1} appears intermediate between the two observed rate constants for the fast (~7 s^{-1}) and slow (0.4 s^{-1}) phases for both 340 nm and 412 nm.

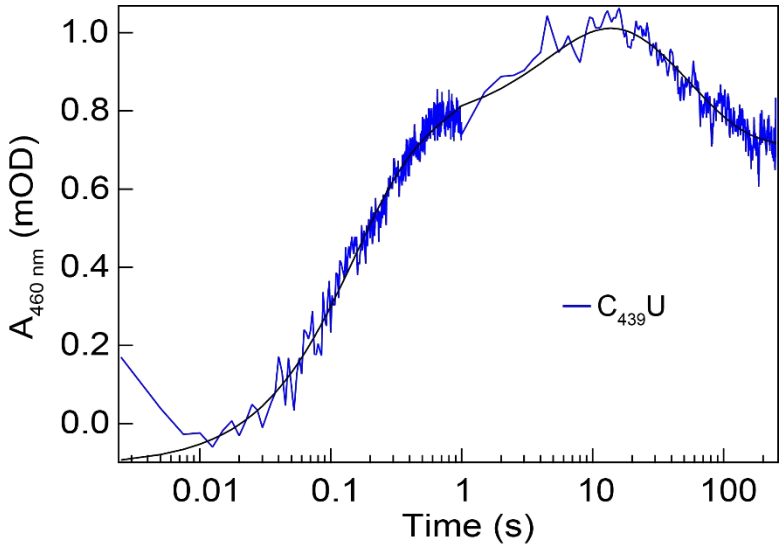

Figure S6. Long timescale stopped-flow kinetics for $C_{439}U$ (blue) α_2 mixing with wt β_2 to a final concentration of 20 μM $\alpha_2\beta_2$, 1 mM CDP and 3 mM ATP in assay buffer monitored at 460 nm.

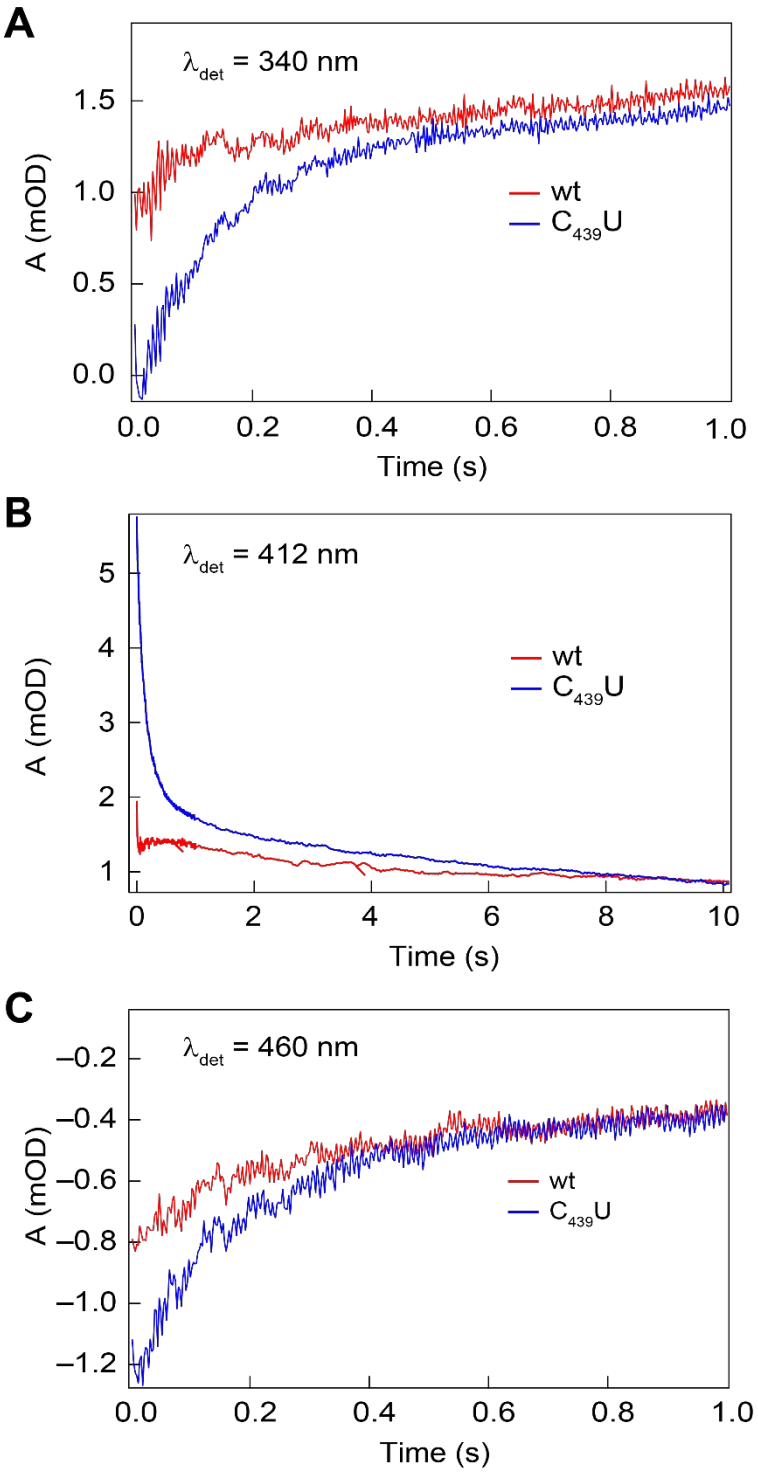

Figure S7. Stopped-flow kinetic comparison between wt (red) and $C_{439}U$ (blue) α_2 mixing with wt β_2 to a final concentration of 20 μM $\alpha_2\beta_2$, 1 mM CDP and 3 mM ATP in assay buffer. Transients recorded at **A** 340 n, **B** 412 nm, and **C** 460 nm. The kinetics of induced absorption (**A** and **C**) and decay (**B**) were again described well by a biexponential function with statistically identical kinetics to those reported at 10 μM $\alpha_2\beta_2$.

Table S3. Fitting parameters for SF UV-vis experiments.

α	λ / nm	A_1 / μOD	k_1 / s^{-1}	A_2 / μOD	k_2 / s^{-1}	A_3 / μOD	k_3 / s^{-1}
$C_{439}U$#	340	570 (20)	6.5 (0.3)	360 (20)	0.42 (0.03)		
	410	–1,580 (20)	7.1 (0.1)	-400 (40)	0.40 (0.01)		
	460	440 (10)	3.19 (0.05)				
$C_{439}U$*	460	770 (10)	7.1 (0.2)	490 (20)	0.44 (0.04)	-430 (20)	0.044 (0.01)
WT*	340	520 (10)	2.9 (0.2)				
	412			-670 (10)	0.29 (0.01)		
	460	400 (10)	3.2 (0.1)				

Experiments performed at 10 μM final concentration.

* Experiments performed at 20 uM final concentration.

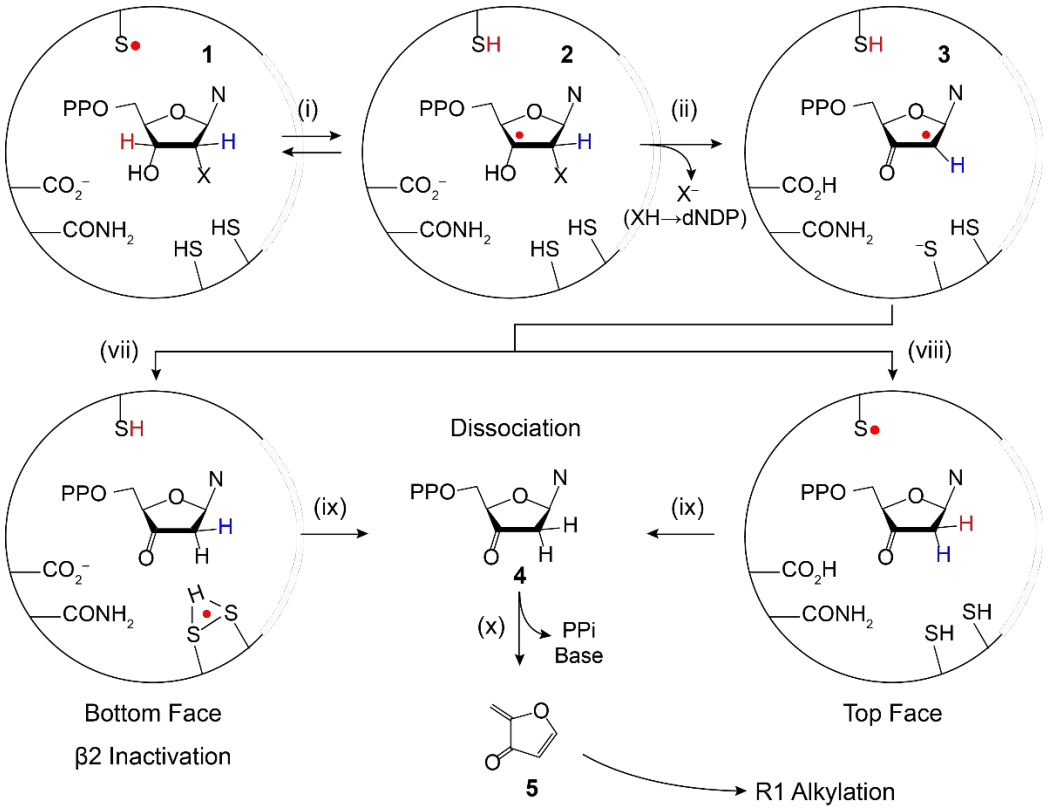

Figure S8. Mechanism of inactivation of RNR by mechanism-based inhibitors 2′-deoxy-2′-X NDP (X = F or Cl). The mechanism of inactivation depend on the nature of substrate radical reduction (steps vii vs. viii). During radical substrate reduction from the top face, α_2 is inactivated through alkylation of the essential sulfhydryl groups by **5**, but the thiyl, and thus the essential Y_{122}• in β, are maintained. Conversely, reduction by the bottom face inactivates both α_2 and β_2 by trapping on the bottom face.

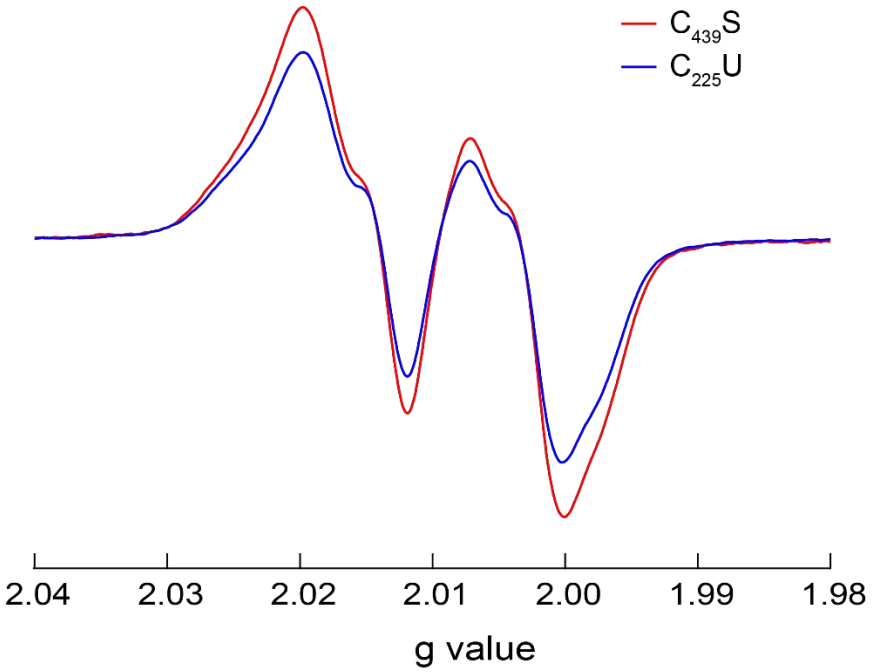

Figure S9. X-band EPR spectrum of 50 μM wt β_2 quenched at 10 s after mixing with 1 mM CDP, 3 mM ATP, and $C_{225}U$ (blue) or $C_{439}S$ (red) α_2. Spectra recorded at 80 K with 1 Gauss modulation amplitude, 100 kHz modulation frequency, and 20 μW microwave power.

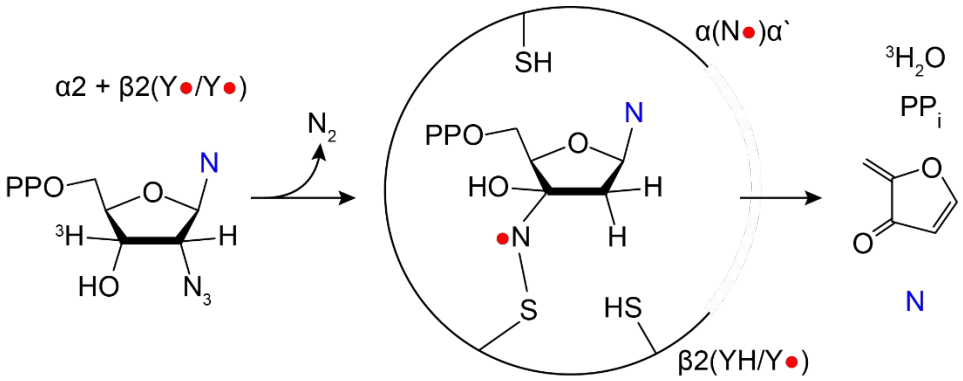

Figure S10. Mechanism of RNR inhibition by N_3NDP.